

C.P. No. 674

LIBRARY
ROYAL AIRCRAFT ESTABLISHMENT
BEDFORD.

C.P. No. 674



MINISTRY OF AVIATION

AERONAUTICAL RESEARCH COUNCIL

CURRENT PAPERS

Forces on Tethered Ballistic Missiles
Due to
Motor Cut-Off - A Theoretical Treatment

By

D. Moxon

LONDON: HER MAJESTY'S STATIONERY OFFICE

1964

Price 6s. 6d. net

August, 1960

FORCES ON TETHERED BALLISTIC MISSILES DUE TO MOTOR
CUT-OFF - A THEORETICAL TREATMENT

by

D. Moxon

SUMMARY

Motor-running tests may be carried out on a ballistic missile while it is tethered to its launcher. When the motors are cut-off the missile structure is excited in various vibration modes by the combined influence of the decaying thrust and the elastic force from the launcher. These vibrations result in loads on the missile which can exceed those encountered in normal flight. It is the magnitude of these loads and the parameters which affect them that are investigated in this paper.

The first part of the paper gives results obtained on the assumption that the missile itself is rigid while the launcher structure is elastic. This is followed by an investigation in which missile flexibility is taken into account. The results in both cases are similar; a high launcher stiffness and a low rate of thrust cut-off are found to be favourable. The effect of fuel load is studied briefly. It is found that as the fuel load decreases the overall forces decrease.

LIST OF CONTENTS

	<u>Page</u>
1 INTRODUCTION	5
2 STATEMENT OF PROBLEM	6
3 PRELIMINARY INVESTIGATION - MISSILE ASSUMED RIGID	6
3.1 Assumptions	6
3.2 Full fuel case	7
3.3 Other fuel cases	19
4 CALCULATIONS - MISSILE ASSUMED FLEXIBLE	11
4.1 Assumptions	11
4.2 Theory	11
4.3 Results - full fuel cases	14
4.4 Results - other fuel cases	17
5 CONCLUDING REMARKS	18
LIST OF SYMBOLS	18
APPENDICES 1-3	20-26
TABLES 1-5	-
ILLUSTRATIONS - Figs. 1-9	-
DETACHABLE ABSTRACT CARDS	-

LIST OF APPENDICES

<u>Appendix</u>			
1	-	Solution of equation of motion - missile rigid	20
2	-	Solution of equations of motion - missile flexible	22
3	-	Analysis of system in which only the thrust structure and launcher are assumed flexible	26

LIST OF TABLES

<u>Table</u>			
1	-	Peak forces in thrust structures	15
2	-	Peak accelerations in fuel tank	15
3	-	Peak forces in fuel tank walls	16
4	-	Variation with fuel content of the maximum force in the fuel tank walls and maximum acceleration of the oxidant tank	17
5	-	Variation of maximum force in thrust structure with fuel content	18

LIST OF ILLUSTRATIONS

	<u>Fig.</u>
Schematic diagram of missile and launcher	1
Comparison of an actual thrust-decay curve with the analytical representation	2
Maximum absolute acceleration against the frequency ratio ω/v (missile rigid)	3
Maximum absolute acceleration against the frequency ratio ω/v ; the effect of fuel load (missile rigid)	4
Mass - spring representation of missile and launcher	5
Effect of rate of motor cut-off on forces on missile (missile flexible)	6
Effect of missile flexibilities on maximum force in thrust structure	7
Effect of launcher stiffness on maximum force in thrust structure (thrust structure flexible, fuel tank walls rigid)	8
Effect of stiffness of thrust structure on maximum force in thrust structure (thrust structure flexible, fuel tank walls rigid)	9

1. INTRODUCTION

The motors of a ballistic missile may be tested while the missile is tethered to its launcher. The thrust of the motors is reacted by the elastic force from the launcher. As soon as the thrust is decreased the equilibrium is disturbed and a vibratory motion commences. This motion involves longitudinal compressive and extensional deformations of the skin of the missile body as well as the deformation associated with the launcher. It is this motion and the resultant elastic and inertia forces that are the subject of this paper.

A simple example will suffice to show that these forces can be quite large. Consider the case of the missile Blue Streak, which has a thrust at launch equal to 1.3 times the all-up weight. If this thrust is abruptly cut, the missile (assumed rigid) begins to move downwards with an acceleration of 1.3g. Since the motion will be very nearly simple harmonic it follows that the acceleration at the lowest point of the motion must be 1.3g, but upwards. Thus, when the effect of gravity is taken into account, the total force supplied by the launcher - and reacted by the missile - is 0.3 A.U.W. downwards at the top of the motion and 2.3 A.U.W. upwards at the bottom of the motion. This would clearly be a more adverse design case than launch, at which the maximum longitudinal acceleration is only 1.3g absolute. The calculations recorded in this paper, however, show that accelerations as high as this would not occur at finite rates of motor cut-off.

A preliminary estimate of the effect of finite rates of motor cut-off is made on the assumption that the missile is rigid. A significant parameter is found to be the ratio of the inverse of the cut-off time to the frequency of the missile on the launcher. As would be expected the forces increase as this ratio increases. This preliminary investigation is followed by a calculation in which the effect of missile flexibility is taken into account.

In these latter calculations the missile is represented, for ease of calculation, by a mass-spring system consisting of two masses and two springs. The launcher is represented as a spring, so the assumed representation has three degrees-of-freedom. The solutions to this system are obtained by the use of the Laplace transformation technique. General expressions are given for the spring extensions and the accelerations of the masses. These quantities are readily convertible into forces and stresses in the missile.

For a particular missile and launcher and a particular rate of shut-off the expressions for the forces become functions of time only. In this work structural damping is ignored so these expressions give a series of peak forces whose magnitude does not decrease with time. It is thought that the effect of structural damping would be to progressively reduce these peaks. If the structural damping is small - as is likely - the rate of reduction from one peak to the next would be small. Since, in fact, even when there is no structural damping one of the first few peaks is found to be always either the highest or very close to the highest peak, we may conclude that the value of the highest peak would not be very significantly affected by structural damping.

Results for the flexible missile are similar to the ones for the rigid missile, though, in general, the forces are a little less. High launcher stiffness, low rate of shut-off and low fuel content are again found to be favourable.

The numerical results given in this paper are based on early estimates for the missile Blue Streak. The present launcher stiffness is, however,

much stiffer than the one taken in these calculations and so the results have no direct application. Nevertheless, it is thought that the results and the analysis may be of interest.

2 STATEMENT OF PROBLEM

The missile and launcher to be analysed are shown schematically in Fig.1. The main components of the missile, from front to rear, are war-head, equipment bay, oxidant tank, fuel tank, thrust structure, motor beams and motors. In flight the thrust from the two motors is transmitted through the motor beams to the base of the thrust structure; but for testing purposes the thrust is reacted at the end of the motor beams at four lugs, which are held in the release mechanism of the launcher. Base beams attach the release mechanism to the ground. Two values of motor cut-off times will be considered, 100 milliseconds and 50 milliseconds. These times are measured from 90% to 10% thrust when the rate of thrust decay is roughly constant. These cut-offs will hereafter be referred to as the slow and rapid cut-off respectively.

The basic problem is to determine the forces experienced by the various parts of the missile in the slow and rapid cut-off. Theory might also indicate how these forces could be reduced if the need arose.

3 PRELIMINARY INVESTIGATION - MISSILE ASSUMED RIGID

In this section the missile is assumed rigid, and a preliminary estimate is made of the effects of rate of motor cut-off and the launcher stiffness on the maximum acceleration. Also certain general principles are established which will be of value in interpreting the results obtained when missile flexibilities are taken into account in a later section.

3.1 Assumptions

The missile is represented as a rigid mass and the launcher as a weightless spring. Structural damping and fuel sloshing are ignored.

The variation of the motor thrust, T , with time t is approximated to by the equation

$$T = \begin{cases} \frac{T_0}{2} (1 + \cos \omega t) & 0 \leq t \leq \pi/\omega \\ 0 & t \geq \pi/\omega \end{cases} \quad (1)$$

where T_0 is the thrust at the beginning of cut-off and ω is a constant for a given rate of out-off and is referred to as the cut-off frequency. For the rapid out-off ω is 37.1 rads/sec and for the slow out-off is 18.5 rads/sec. Fig.2 shows a comparison between a true out-off curve and the analytical representation.

3.2 Full fuel case

The missile mass, launcher stiffness and rate of motor cut-off are treated as variables in this analysis.

If m is the mass of the missile in slugs

k is the stiffness of the launcher in lb/ft

T_0 is the thrust of the motors in lb force

x is the upward displacement of the missile from the equilibrium position for zero thrust

t is the time in secs measured from the time at which the motors start to be cut-off

then the equation of motion is

$$m\ddot{x} + kx = \begin{cases} \frac{T_0}{2} (1 + \cos \omega t) & 0 \leq t \leq \pi/\omega \\ 0 & t \geq \pi/\omega \end{cases} \quad (2)$$

The solution (derived in Appendix 1) and its first three derivatives is

$$\left. \begin{aligned} x &= \frac{\ell}{2} \left\{ 1 + \frac{1}{\nu^2 - \omega^2} \left(\nu^2 \cos \omega t - \omega^2 \cos \nu t \right) \right\} \\ \dot{x} &= \frac{\ell \nu \omega}{2(\nu^2 - \omega^2)} \left\{ -\nu \sin \omega t + \omega \sin \nu t \right\} \\ \ddot{x} &= \frac{\ell \nu^2 \omega^2}{2(\nu^2 - \omega^2)} \left\{ -\cos \omega t + \cos \nu t \right\} \\ \dddot{x} &= \frac{\ell \nu^2 \omega^2}{2(\nu^2 - \omega^2)} \left\{ \omega \sin \omega t - \nu \sin \nu t \right\} \end{aligned} \right\} 0 \leq t \leq \pi/\omega \quad (3a)$$

$$\left. \begin{aligned} x &= -\frac{\ell \omega^2}{2(\nu^2 - \omega^2)} \left\{ \cos \nu t + \cos \nu (t - \pi/\omega) \right\} \\ \dot{x} &= \frac{\ell \nu \omega^2}{2(\nu^2 - \omega^2)} \left\{ \sin \nu t + \sin \nu (t - \pi/\omega) \right\} \\ \ddot{x} &= \frac{\ell \nu^2 \omega^2}{2(\nu^2 - \omega^2)} \left\{ \cos \nu t + \cos \nu (t - \pi/\omega) \right\} \\ \dddot{x} &= \frac{-\ell \nu^3 \omega^2}{2(\nu^2 - \omega^2)} \left\{ \sin \nu t + \sin \nu (t - \pi/\omega) \right\} \end{aligned} \right\} t \geq \pi/\omega \quad (3b)$$

where

l is the displacement from the equilibrium position at $t = 0$ and is given by T/k

ν is the natural frequency of the missile on the launcher and is

given by $\{k/m\}^{1/2}$ rads/sec.

When $\nu = \omega$ the above expressions are indeterminate; however, de d'Hospital's rule for finding the limit as $\nu \rightarrow \omega^*$ enables the solution to be written down at once. The solution is

$$\left. \begin{aligned} x &= \frac{l}{2} \left\{ 1 + \cos \omega t + \frac{\omega t}{2} \sin \omega t \right\} \\ \dot{x} &= \frac{l\omega}{4} \left\{ -\sin \omega t + \omega t \cos \omega t \right\} \\ \ddot{x} &= -\frac{l\omega^2}{4} \left\{ \omega t \sin \omega t \right\} \\ \dddot{x} &= -\frac{l\omega^3}{4} \left\{ \omega t \cos \omega t + \sin \omega t \right\} \end{aligned} \right\} 0 \leq t \leq \pi/\omega \quad (4a)$$

$$\left. \begin{aligned} x &= \frac{l\pi}{4} \sin \omega t \\ \dot{x} &= \frac{l\omega\pi}{4} \cos \omega t \\ \ddot{x} &= -l\omega^2 \frac{\pi}{4} \sin \omega t \\ \dddot{x} &= -l\omega^3 \frac{\pi}{4} \cos \omega t \end{aligned} \right\} t \geq \pi/\omega \quad (4b)$$

If the ratio of the full thrust to the weight of the missile is denoted by 'f', then $l (= T/k)$ can be written as fg/ν^2 . If this expression for l is substituted in equations (3a) and (3b) the acceleration is seen to depend on f and the ratio ω/ν . For the missile, Blue Streak, $f = 1.3$ for the full fuel case. For this particular value of f, the variation of the maximum absolute acceleration with ω/ν is obtained.

* If $f(a) = g(a) = 0$

$$\lim_{x \rightarrow a} \frac{f(x)}{g(x)} = \lim_{x \rightarrow a} \frac{f'(x)}{g'(x)}$$

In this connection it should be realised that \ddot{x} is the acceleration relative to gravity. To get the absolute acceleration - and this is what determines the inertia forces - g must be added to \ddot{x} . For this reason only the maximum values of \ddot{x} are thought to be of interest.

In these calculations what is required ideally is an analytical relationship between \ddot{x}_{\max} and ω/ν ; but this is not possible except for certain values of ω/ν . Instead \ddot{x}_{\max} will be determined for a series of specific frequency ratios. The stationary values of \ddot{x} occur when $\dot{\ddot{x}}$ is zero. The approximate roots of $\ddot{x} = 0$ can be found graphically; the more exact roots can then be found by interpolating near these approximate roots. As \ddot{x}_{\max} only is required only the alternate roots need be found. A plot of the maximum absolute acceleration experienced by the missile against ω/ν is given in Fig.3.

The stiffness of the Blue Streak launcher was expected to be about 21.8×10^6 lb/ft and the mass of the missile is 6428.6 slugs. This gives $\nu = 58.2$ rads/sec. Hence the rapid cut-off corresponds to $\omega/\nu = 0.64$, and the slow cut-off to $\omega/\nu = 0.32$. It will be seen from Fig.3 that these ratios correspond to accelerations of 1.69g and 1.1g respectively. To decrease the rate of cut-off or to increase the launcher stiffness is clearly beneficial.

For certain values of ω/ν an analytical expression can be obtained for \ddot{x}_{\max} in terms of ω/ν . Consideration of these and certain other cases leads to a more complete understanding of Fig.3. Consider the following cases.

(i) $\nu/\omega = R_E$, an even integer

Equations (3a) show that at time $t = \pi/\omega$, x achieves its maximum negative value. The lowest point of the motion is therefore reached at the time when the thrust first becomes zero. The maximum acceleration also occurs at this time, the time-dependent part of the expression for \ddot{x} attaining its maximum possible value of 2. The maximum acceleration in this case is therefore given by

$$\ddot{x}_{\max} = \frac{1.3g}{R_E^2 - 1} .$$

This value will be reached every cycle in the S.H.M. which prevails when $t > \pi/\omega$.

(ii) $\nu/\omega = R_O$, an odd integer other than 1

Equations (3a) show that at time $t = \pi/\omega$, $x = \dot{x} = 0$; and so the missile comes to rest when the thrust becomes zero. However, the time-dependent part of the expression for \ddot{x} must be less than 2, and so

$$\ddot{x}_{\max} < \frac{1.3g}{R_O^2 - 1} .$$

This shows that the curve in Fig.3, although it appears smooth, has, in fact, a small amplitude 'wave' on it. This effect is clearly not important for the rigid missile.

(iii) $\nu/\omega = R$, any number less than 1

At $t = \pi/\omega$, x is positive and \dot{x} is negative. There can only be one root of $\ddot{x} = 0$ between $t = 0$ and $t = \pi/\omega$ and this must represent a minimum \ddot{x} . The greatest positive acceleration must therefore occur at the lowest point in the S.H.M. and this is given by

$$\ddot{x}_{\max} = \frac{1.3g}{1 - R^2} \cos\left(\frac{R\pi}{2}\right).$$

(iv) $\nu/\omega = 1$

Equations (4a) show that at $t = \pi/\omega$, $x = 0$ and \dot{x} is negative. Since there can only be one stationary value of \ddot{x} up to $t = \pi/\omega$ this must be a minimum. The maximum positive value of the acceleration must therefore occur at the lowest point of the S.H.M. and is given immediately by equation (4b) as

$$\ddot{x}_{\max} = \ell \omega^2 \frac{\pi}{4} = \frac{1.3\pi g}{4}.$$

Note that if the specified thrust variation were unrestricted with respect to time, the amplitude of the motion would grow with time, since equations (2a) would describe the complete motion; this corresponds, of course, to the familiar 'peaking' of response curves that occurs when the frequency of the exciting force approaches a natural frequency of the system. That there is no peak at $\omega/\nu = 1$ in Fig.3 is due to the fact that the thrust is restricted to half a cycle. Moreover, it can be shown that the missile moves downwards all the time that the thrust is acting and so the thrust must extract energy from the system.

3.3 Other fuel cases

It was seen in the last section that the maximum acceleration depends on the ratio of the motor thrust to the mass of the missile, and the ratio of the cut-off frequency to the natural frequency of the missile on its launcher. The former ratio was called f and the latter ω/ν . For any specific value of ω/ν then the maximum acceleration is inversely proportional to the mass. This fact and the results plotted in Fig.3 enables curves of \ddot{x}_{\max} against ω/ν to be determined immediately for any mass. Curves of $g + \ddot{x}_{\max}$ against ω/ν are shown in Fig.4 for missile masses m_0 , $0.8 m_0$, $0.6 m_0$, $0.4 m_0$ and $0.1 m_0$, where m_0 is the mass of the missile in the full fuel condition.

For any specific shut-off rate and launcher stiffness ω/ν is proportional to the square root of the missile mass. The variation of the absolute maximum acceleration with the missile mass is therefore given in Fig.4 by curves which are not vertical but which bend towards the lower values of ω/ν as the mass decreases. Three such curves are shown in Fig.4, the one to the left is appropriate to the rapid cut-off rate and the expected launcher stiffness. A curve appropriate to the slow cut-off rate and the expected launcher stiffness would be further to the left.

With reference to Fig.4, it should be noted that the force in the launcher and thrust structure is not proportional to the acceleration, since

the mass is continuously varying along the dashed curves. The force is, in fact, given by the product of the mass and the acceleration; and inspection of Fig.4 will indicate that the force always decreases as the mass decreases. Missile components whose mass remains constant (e.g. the propulsive unit, the equipment bay and warhead) will be subjected to forces proportional to the acceleration. However, this is of no concern at any likely rate of shut-off or launcher stiffness, since these parts are designed to withstand the very high g's that are encountered in flight.

To summarise: the overall forces decrease with decrease in fuel weight; the acceleration may rise a little, but this is of no concern.

4 CALCULATIONS - MISSILE ASSUMED FLEXIBLE

In the calculations recorded in the last section the missile was assumed rigid and so each part of the missile necessarily suffered the same acceleration. In this section missile flexibilities will be taken into account, so different parts of the missile may be expected to experience different accelerations. The accelerations and elastic forces associated with this more complex motion will now be determined. This determination is the most important part of the whole investigation.

4.1 Assumptions

The missile and launcher will be assumed to deform in a semi-rigid manner. Three possible modes of deformation of the missile would be: (i) extension of the thrust structure, (ii) extension of the fuel tank walls, (iii) extension of the oxidant tank walls. In fact mode (iii) will be ignored as its frequency in the full fuel condition is expected to be high in comparison with the frequencies of modes (i) and (ii) and it should also be well above the frequency of the launcher. (In the calculations on the rigid missile, it will be remembered, the full fuel condition was found to be the most critical). Another frequency that is expected to be high is that of the motors on the motor beams and this flexibility will also be ignored.

The inertia of the thrust structure in mode (i) will be ignored; the thrust structure then becomes effectively a weightless spring. Similarly the fuel tank walls will be represented by a weightless spring between the fuel tank and the oxidant tank. As in the calculations on the rigid missile, the inertia of the launcher, structural damping and fuel sloshing will be ignored. Also the motor thrust will be represented by the same analytical expression.

4.2 Theory

Fig.5 shows the mass-spring representation of the missile and launcher. The top mass represents the mass of the missile forward of the middle diaphragm, and a very large part of this mass for the full fuel condition will be the liquid oxygen. The lower mass represents the mass of the fuel and fuel tank. Springs (1), (2) and (3) represent the flexibilities in the launcher, the thrust structure and the fuel tank walls respectively. The motor thrust acts between the two lower springs and will be looked upon as acting at a weightless diaphragm.

What is required from this calculation is the greatest elastic forces in springs (2) and (3) and the greatest accelerations of the two masses. The greatest forces in springs (2) and (3) will be obtained by finding the greatest compression of each spring. The greatest acceleration of the top mass can be deduced at once from the greatest force in spring (3). The acceleration of the lower mass is given by differentiating its displacement twice with respect to time.

With these requirements in view, let us take the three generalised co-ordinates of the system to be extensions of the three springs; the equilibrium position at zero thrust will be taken as the datum. Also let

$m(1-\beta)$ be the mass in slugs of the upper mass

$m\beta$ " " " " " " " lower "

(where β is a constant depending only on the ratio of the two masses)

k_1 be the stiffness of spring (1) in lb/ft

k_2 " " " " " (2) " "

k_3 " " " " " (3) " "

x_1 be the extensions of spring (1) in ft

x_2 " " " " " (2) " "

x_3 " " " " " (3) " "

Then the kinetic energy of the system is given by

$$\frac{1}{2}(1-\beta) m(\dot{x}_1 + \dot{x}_2 + \dot{x}_3)^2 + \frac{1}{2}\beta m(\dot{x}_1 + \dot{x}_2)^2$$

and the potential energy by

$$\frac{1}{2}(k_1 x_1^2 + k_2 x_2^2 + k_3 x_3^2).$$

The Lagrangian equations of motion then are:-

$$(1-\beta) m(\ddot{x}_1 + \ddot{x}_2 + \ddot{x}_3) + k_3 x_3 = 0. \quad (5)$$

$$\beta m(\ddot{x}_1 + \ddot{x}_2) + (1-\beta) m(\ddot{x}_1 + \ddot{x}_2 + \ddot{x}_3) + k_2 x_2 = 0. \quad (6)$$

$$\beta m(\ddot{x}_1 + \ddot{x}_2) + (1-\beta) m(\ddot{x}_1 + \ddot{x}_2 + \ddot{x}_3) + k_1 x_1 = \frac{T_0}{2} (1 + \cos \omega t). \quad (7)$$

These three equations enable the three generalised co-ordinates to be separated and so differential equations can be formed in terms of x_2 , x_3 and $x_1 + x_2$ separately. This last quantity, $x_1 + x_2$, which, when differentiated twice with respect to time, gives the acceleration of the lower mass, is hereafter referred to as x_β .

The solutions for x_2 , x_3 and \ddot{x}_β (derived in Appendix 2) are given below. The amount by which the forces in springs (2) and (3) are greater than those at datum are given by $-k_2 x_2$ and $-k_3 x_3$ respectively.

$$x_2 \quad (0 \leq t \leq \pi/\omega) = \frac{\ell \omega^2 k_1}{2(k_1 + k_2)} \left\{ (\tau - \omega^2) E_1 + \frac{\cos rt}{s^2 - r^2} + \frac{\cos st}{r^2 - s^2} \right\} \quad (8a)$$

$$x_2 \quad (t > \pi/\omega) = \frac{\ell \omega^2 k_1}{2(k_1 + k_2)} \left\{ 2(\tau - \omega^2) E_2 + \frac{\cos rt}{s^2 - r^2} + \frac{\cos st}{r^2 - s^2} \right\} \quad (8b)$$

$$x_3 \quad (0 \leq t \leq \pi/\omega) = \frac{\ell \omega^2 k_1 k_2}{2\beta m (k_1 + k_2)} \cdot E_1 \quad (9a)$$

$$x_3 \quad (t > \pi/\omega) = \frac{\ell \omega^2 k_1 k_2}{2\beta m (k_1 + k_2)} \cdot 2E_2 \quad (9b)$$

$$\ddot{x}_\beta \quad (0 \leq t \leq \pi/\omega) = \frac{\ell \gamma}{2} \left\{ -\frac{(\cos rt - \cos st)}{r^2 - s^2} + \left(1 - \frac{\omega^2}{\beta \tau}\right) \frac{d^2 E_1}{dt^2} + \frac{\ell}{r^2 - s^2} \left\{ (\alpha r^2 - r^4) \cos rt - (\alpha s^2 - s^4) \cos st \right\} \right\} \quad (10a)$$

$$\ddot{x}_\beta \quad (t > \pi/\omega) = \ell \gamma \left\{ \frac{\sin r(t - \pi/2\omega) \sin r\pi/2\omega - \sin s(t - \pi/2\omega) \sin s\pi/2\omega}{r^2 - s^2} + \left(1 - \frac{\omega^2}{\beta \tau}\right) \frac{d^2 E_2}{dt^2} \right\} + \frac{\ell}{r^2 - s^2} \left\{ (\alpha r^2 - r^4) \cos rt - (\alpha s^2 - s^4) \cos st \right\} \quad (10b)$$

where r and s are the natural periods of vibration of the mass-spring system and are given by

$$\frac{r^2}{s^2} = \frac{\alpha \pm \sqrt{\alpha^2 - 4\gamma}}{2}$$

$$\alpha = -\frac{1}{\beta m} \left\{ \frac{k_3}{(1 - \beta)} + \frac{k_1 k_2}{k_1 + k_2} \right\}$$

$$\gamma = \frac{k_1 k_2 k_3}{m^2 \beta (1 - \beta) (k_1 + k_2)}$$

$$e = T_0 / k_1$$

$$\tau = \frac{k_3}{m\beta(1-\beta)}$$

$$E_1 = \frac{\cos \omega t}{(r^2 - \omega^2)(s^2 - \omega^2)} + \frac{\cos r t}{(\omega^2 - r^2)(s^2 - r^2)} + \frac{\cos s t}{(\omega^2 - s^2)(r^2 - s^2)}$$

$$E_2 = \frac{\cos r(t - \pi/2\omega) \cos r\pi/2\omega}{(\omega^2 - r^2)(s^2 - r^2)} + \frac{\cos s(t - \pi/2\omega) \cos s\pi/2\omega}{(\omega^2 - s^2)(r^2 - s^2)}$$

ω and m have the same meanings as before.

When specific values of mass, stiffness, motor thrust and rate of motor cut-off are substituted into these expressions, expressions are obtained in which t is the only variable. The turning points of the three expressions are given by the roots of $\dot{x}_2 = 0$, $\dot{x}_3 = 0$ and $\ddot{x}_\beta = 0$. Since negative values of x_2 and x_3 increase the already compressive spring forces it is assumed that the maximum force in springs (2) and (3) will occur at minimum values of x_2 and x_3 . Therefore the roots corresponding to minimum values only will be calculated. Also only the maximum values of \ddot{x}_β will be found, as the absolute acceleration is given by $g + \ddot{x}_\beta$. The required roots will be found by the method used in the calculations on the rigid missile and described in Section 3.2.

4.3 Results - full fuel case

The following values, based on early estimates for Blue Streak, are used. The estimated launcher stiffness, k_1 , is considerably less than that of the present Blue Streak launcher.

$$\begin{aligned} \beta &= 0.372 \\ k_1 &= 21.8 \times 10^6 \text{ lb/ft} \\ k_2 &= 42 \times 10^6 \text{ lb/ft} \\ k_3 &= 24 \times 10^6 \text{ lb/ft} \\ T_0 &= (207,000)(1.3) \text{ lb} \\ m &= 6428.6 \text{ slugs} \end{aligned}$$

These values give normal mode frequencies, r and s , of 14.2 and 42.0 rads/sec. The rate of motor cut-off is left as a parameter.

In the results that follow the elastic forces are expressed as a proportion of the static force. Forces arising from any internal pressure are not included in either the elastic or static force. The static force

* The actual value of the k_2 might be nearer 36 than 42. It will be shown that this change in k_2 does not have much effect on the forces.

in the fuel tank walls (spring (3)), for example, is equal to the weight of liquid oxygen and its tank, the equipment bay and warhead. The values of the first few peak forces and accelerations experienced by the different parts of the missile are given below for a range of motor cut-off times. The figures in round brackets are the values of the maximum possible peaks that could occur if structural damping were really absent and the motion went on indefinitely. The figures in square bracket are the corresponding figures for $k_2 = 36$ instead of 42.

TABLE 1

Peak forces in thrust structure

Cut-off time in millisecs (90% - 10% thrust)	Peak forces in thrust structure \div 207,000 lb			
	1st peak	2nd peak	3rd peak	All-time maximum
29.5	1.50	1.60	1.57	(1.61)
36.9	1.52	1.58	1.59	(1.60)
59.0	1.45	1.42	1.44	(1.45)
98.3				(1.17)

TABLE 2

Peak accelerations of fuel tank

Cut-off time in millisecs (90% - 10% thrust)	Peak accelerations of fuel tank \div g			
	1st peak	2nd peak	3rd peak	All-time maximum
29.5				(1.86)
36.9				(1.51)
59.0	0.89	1.36	1.39	(1.40)
98.3				(1.15)

TABLE 3

Peak forces in fuel tank walls

Cut-off time in milliseconds (90%-10% thrust)	Peak forces in fuel tank walls ÷ 130,000 lb					
	1st peak	2nd peak	3rd peak	4th peak	All-time max.	All-time max. (k ₂ = 36)
29.5	0.38	1.46	1.75	1.83	(1.83)	[1.80]
36.9	0.52	1.62	1.65	1.60	(1.66)	[1.63]
39.1					(1.61)	
50.0					(1.59)	[1.57]
59.0	0.75	1.49	1.46	1.50	(1.50)	[1.49]
65.2					(1.43)	
74.0					(1.38)	
86.0					(1.27)	
98.3					(1.18)	[1.19]

Figures for the peak accelerations ÷ g of the oxidant tank, equipment bay and warhead are the same as those immediately above. The above peak values occur about 7 times/sec; this corresponds roughly with the lowest natural frequency of the system.

It will be seen that the maximum value, given in brackets, is quite a good indication of the greatest peak value that occurs in the early cycles. In view of this it would seem justifiable in preliminary calculations of this nature to calculate only this maximum, and so reduce the computation.

These maxima are far easier to calculate than the first few peaks. The greatest force (elastic or inertia) that can occur in any member after the thrust has ceased to act is given by the sum of the peak forces experienced by that member in each of the normal modes. The reason for this is that these peak forces must eventually coincide - or very nearly so - since the two normal modes will, in general, be of different frequency. This force will usually be the greatest that occurs in the complete motion; but it is possible that a greater force will occur before the thrust has ceased to act. The maximum forces quoted above in brackets are the greatest forces that occur in the complete motion.

Fig. 6 shows a plot of these maxima against the motor cut-off time. For a rapid cut-off a maximum force of about 1.52 (207,000) lb is estimated in the thrust structure. The actual maximum force (longitudinal) in the fuel tank walls is estimated to be about 1.59 (130,000) lb less the force due to internal pressure. The estimated maximum acceleration of the fuel tank is 1.46g, and that of the oxidant tank, equipment bay and warhead is 1.59g. The forces and accelerations for a slow motor cut-off are all much less.

The above values for the forces in the thrust structure and the acceleration of the fuel tank are based on the assumption that the variations with cut-off time are smooth. The force in the fuel tank walls is, in fact, shown to vary quite smoothly with the motor cut-off time for cut-off time between 50 and 100 milliseconds. The reason for the kinks in this 'curve' at cut-off times in the region of 40 and 65 milliseconds can be seen from equation 9b. Cut-off times of 39.1 and 65.2 milliseconds correspond to $\omega = r/3$ and $r/5$ respectively; and it will be seen from equation 9b that, when ω has these values, the force contribution from the normal mode of frequency r is zero for all times greater than π/ω . This tends to level the maximum force curve in these regions.

It is of interest to compare the results plotted in Fig.6 with those that are obtained when the missile is allowed only one flexibility, that of the thrust structure. The expressions for the motion in this case are much simpler and their derivation is given in Appendix 3. From these expressions the maximum force in the thrust structure has been determined at a series of cut-off rates; the graph is shown in Fig.7. Also plotted in Fig.7 are the corresponding results for the rigid missile and the results for the missile with two flexibilities.

This simple representation has also been used to estimate the effect of stiffness changes in the launcher and thrust structure. For a specific cut-off time, 59.5 milliseconds, graphs have been obtained of the maximum force in the thrust structure against the launcher stiffness and the stiffness of the thrust structure; these graphs are given in Figs.8 and 9 respectively. Increase in launcher stiffness and decrease in the stiffness of the thrust structure are seen to be beneficial.

4.4 Results - other fuel cases

The forces experienced by the missile in any fuel loading condition are given by equations 8a, 8b, 9a, 9b, 10a and 10b of the last section. As the fuel is burnt m decreases but β may be assumed constant. This assumption will be seriously in error only at very low fuel content. For a specific cut-off time, 59.5 milliseconds, the maximum force in the fuel tank walls and the acceleration of the oxidant tank and head have been determined for a series of missile masses. ('Maximum force' has the same meaning as it had in the last section.) The maximum force in the fuel tank walls is expressed below as a proportion of the static force in the fuel tank walls when the missile is in its full fuel condition.

TABLE 4

Variation with fuel content of the maximum force in the fuel tank walls and maximum acceleration of the oxidant tank

Mass of missile (slugs)	Max force in fuel tank walls ($\div 130,000$ lb)	Max acceleration of oxidant tank and head ($\div g$)
6428.6	1.50	1.50
0.81 (")	1.24	1.53
0.49 (")	0.78	1.59
0.1 (")	0.14	1.44

The effect of fuel loading on the force in the thrust structure has been determined only by the two-degree-of-freedom analysis described at the end of the last section. The results obtained for a motor cut-off time of 59.5 milliseconds are given below. The maximum force in the thrust structure is expressed as a proportion of static for the full fuel condition.

TABLE V

Variation of max force in thrust structure
with fuel content

Mass of missile (slugs)	Max force in thrust structure (+ 207,000 lb)
6428.6	1.48
0.81 (")	1.23
0.49 (")	0.72
0.1 (")	0.14

It will be seen that the results from both these calculations are quite similar to the results obtained for the rigid missile for the rapid rate of cut-off: the overall force decreases with decrease in fuel content but the acceleration may increase a little. In view of this a more elaborate investigation was thought to be unnecessary.

5 CONCLUDING REMARKS

A rapid shut-down of the motors of a tethered ballistic missile can cause a greater acceleration than that experienced at launch and could govern the design of part of the structure. If the missile is treated as rigid, and we denote the natural frequency of the rigid missile on the launcher by ν rads/sec and the cut-off time (90% - 10% thrust) by $1.85/\omega$ secs, then the maximum acceleration induced by the shut-down was found to depend only on the ratio of ω/ν and the magnitude of the full thrust. In the case of the missile, Blue Streak, the full thrust of which is 1.3 times the all-up-weight, the maximum acceleration increases from 1g to 2g as ω/ν increases from 0 to 1.

Analytical expressions were derived for the forces in a missile treated as flexible. The forces in the missile were then calculated for a particular missile and launcher for a series of motor cut-off times. The results show similar trends to those obtained for the rigid missile, in that the acceleration increases as the cut-off time decreases.

LIST OF SYMBOLS

Symbols used in Section 3:-

- T combined thrust of motors at time t
- T_0 combined thrust of motors before cut-off
- ω motor cut-off frequency (see equation 1)
- m mass of missile
- m_0 mass of missile in full fuel condition
- x upward displacement of missile from equilibrium position for zero thrust
- k stiffness of launcher
- ℓ displacement before cut-off of missile from equilibrium position,
 $\ell = T_0/k$
- f T_0/m
- ν natural frequency of missile on launcher, $\nu = [k/m]^{1/2}$
- R_E ν/ω , an even integer

LIST OF SYMBOLS (CONTD.)

- R_0 ν/ω , an odd integer other than 1
 R ν/ω , where $\nu/\omega < 1$

Additional symbols used in Section 4:-

- r and s natural periods of vibration of the missile-launcher system,

$$\frac{r^2}{s^2} = \frac{\alpha \pm \sqrt{\alpha^2 - 4\gamma}}{2}$$

α $\frac{1}{\beta m} \left\{ \frac{k_3}{1-\beta} + \frac{k_1 k_2}{k_1 + k_2} \right\}$

γ $\frac{k_1 k_2 k_3}{\beta m^2 (1-\beta)(k_1 + k_2)}$

τ $\frac{k_3}{\beta m(1-\beta)}$

E_1 $\frac{\cos \omega t}{(r^2 - \omega^2)(s^2 - \omega^2)} + \frac{\cos r t}{(\omega^2 - r^2)(s^2 - r^2)} + \frac{\cos s t}{(\omega^2 - s^2)(r^2 - s^2)}$

E_2 $\frac{\cos r \left(t - \frac{\pi}{2\omega} \right) \cos \frac{r\pi}{2\omega}}{(\omega^2 - r^2)(s^2 - r^2)} + \frac{\cos s \left(t - \frac{\pi}{2\omega} \right) \cos \frac{s\pi}{2\omega}}{(\omega^2 - s^2)(r^2 - s^2)}$

- | | | | |
|-----------|---|---|---|
| x_1 | extension of launcher | } | all equal to zero in equilibrium position for zero thrust |
| x_2 | extension of thrust structure | | |
| x_3 | extension of fuel tank walls | | |
| x_β | $x_1 + x_2$, displacement of fuel tank | | |
| k_1 | stiffness of launcher (= k) | | |
| k_2 | stiffness of thrust structure | | |
| k_3 | stiffness of fuel tank walls | | |

APPENDIX 1

SOLUTION OF EQUATION OF MOTION - MISSILE RIGID

The equation of motion for the rigid missile is shown in Section 3.2 to be

$$m\ddot{x} + kx = \begin{cases} \frac{T_0}{2} (1 + \cos \omega t) & 0 \leq t \leq \pi/\omega \\ 0 & t \geq \pi/\omega. \end{cases}$$

The boundary conditions are $x = \ell$, $\dot{x} = 0$ at $t = 0$.

Using the fact that $T_0 = k\ell$ and writing k/m as ν^2 the equation becomes

$$\ddot{x} + \nu^2 x = \begin{cases} \frac{\nu^2 \ell}{2} (1 + \cos \omega t) & 0 \leq t \leq \pi/\omega \\ 0 & t \geq \pi/\omega. \end{cases}$$

The Laplace transform of this equation is

$$(p^2 + \nu^2) \bar{x} = \frac{\nu^2 \ell}{2} \left\{ \frac{1}{p} (1 - e^{-\pi p/\omega}) + \frac{p}{p^2 + \omega^2} (1 + e^{-\pi p/\omega}) \right\} + p\ell$$

where \bar{x} is the Laplace transform of x .

Thus

$$\begin{aligned} \bar{x} &= \frac{\nu^2 \ell}{2} \left\{ \frac{(1 - e^{-\pi p/\omega})}{p(p^2 + \nu^2)} + \frac{p(1 + e^{-\pi p/\omega})}{(p^2 + \nu^2)(p^2 + \omega^2)} \right\} + \frac{p\ell}{p^2 + \nu^2} \\ &= \frac{\nu^2 \ell}{2} \left\{ \frac{1}{\nu^2} \left(\frac{1}{p} - \frac{p}{p^2 + \nu^2} \right) (1 - e^{-\pi p/\omega}) + \frac{1}{\omega^2 - \nu^2} \left(\frac{p}{p^2 + \nu^2} - \frac{p}{p^2 + \omega^2} \right) (1 + e^{-\pi p/\omega}) \right\} \\ &\quad + \frac{p\ell}{p^2 + \nu^2} \end{aligned}$$

hence

$$\begin{aligned} x \quad (0 \leq t \leq \pi/\omega) &= \frac{\ell}{2} \left\{ 1 - \cos \nu t + \frac{\nu^2}{\omega^2 - \nu^2} (\cos \nu t - \cos \omega t) + 2 \cos \nu t \right\} \\ &= \frac{\ell}{2} \left\{ 1 + \frac{1}{\nu^2 - \omega^2} (\nu^2 \cos \omega t - \omega^2 \cos \nu t) \right\} \end{aligned}$$

and

$$\begin{aligned}
 x_{(t \geq \pi/\omega)} &= \frac{l}{2} \left\{ 1 - \cos vt - \left[1 - \cos v \left(t - \frac{\pi}{\omega} \right) \right] + \right. \\
 &\quad + \frac{v^2}{\omega^2 - v^2} \left[\cos vt - \cos \omega t + \left(\cos v \left(t - \frac{\pi}{\omega} \right) - \cos \omega \left(t - \frac{\pi}{\omega} \right) \right) \right] + \\
 &\quad \left. + 2 \cos vt \right\} \\
 &= \frac{l \omega^2}{2(\omega^2 - v^2)} \left\{ \cos vt + \cos v \left(t - \frac{\pi}{\omega} \right) \right\} .
 \end{aligned}$$

APPENDIX 2

SOLUTION OF EQUATIONS OF MOTION - MISSILE FLEXIBLE

The equation of motion for this case is derived in Section 4.2. and is

$$(1-\beta) m(\ddot{x}_1 + \ddot{x}_2 + \ddot{x}_3) + k_3 x_3 = 0 \quad (11)$$

$$\beta m(\ddot{x}_1 + \ddot{x}_2) + (1-\beta) m(\ddot{x}_1 + \ddot{x}_2 + \ddot{x}_3) + k_2 x_2 = 0 \quad (12)$$

$$\beta m(\ddot{x}_1 + \ddot{x}_2) + (1-\beta) m(\ddot{x}_1 + \ddot{x}_2 + \ddot{x}_3) + k_1 x_1 = \begin{cases} \frac{T_0}{2} (1 + \cos \omega t) & 0 \leq t \leq \pi/\omega \\ 0 & t > \pi/\omega \end{cases} \quad (13)$$

The boundary conditions are $x_1 = l$, $\dot{x}_1 = \dot{x}_2 = \dot{x}_3 = \dot{x}_\beta = 0$ at $t = 0$.

Equations (11), (12) and (13) enable differential equations to be formed in x_2 , x_3 and $x_1 + x_2 (= x_\beta)$ separately. These equations are

$$\ddot{x}_2 + \alpha \ddot{x}_2 + \gamma x_2 = \begin{cases} \frac{T_0}{2} \{\tau - \omega^2\} \frac{\omega^2 \cos \omega t}{k_1 + k_2} & 0 \leq t \leq \pi/\omega \\ 0 & t > \pi/\omega \end{cases} \quad (14)$$

$$\ddot{x}_3 + \alpha \ddot{x}_3 + \gamma x_3 = \begin{cases} \frac{T_0}{2} \frac{\omega^2 k_2 \cos \omega t}{\beta m (k_1 + k_2)} & 0 \leq t \leq \pi/\omega \\ 0 & t > \pi/\omega \end{cases} \quad (15)$$

$$\ddot{x}_\beta + \alpha \ddot{x}_\beta + \gamma x_\beta = \begin{cases} \frac{T_0 \gamma}{2 k_1} \left\{ 1 + \left(1 - \frac{m(1-\beta)\omega^2}{k_3} \right) \cos \omega t \right\} & 0 \leq t \leq \pi/\omega \\ 0 & t > \pi/\omega \end{cases} \quad (16)$$

where the symbols have the meaning that they have in Section 4.2. The boundary conditions of equations (14), (15) and (16) are determined from the original equations of motion (11), (12) and (13) and their boundary conditions. The boundary conditions of equations (14), (15) and (16) are respectively:-

$$\begin{array}{llllll} x_2 = 0, & \dot{x}_2 = 0, & \ddot{x}_2 = \frac{l\omega^2 k_1}{2(k_1 + k_2)}, & \ddot{x}_2 = 0, & \text{when } t = 0 \\ x_3 = 0, & \dot{x}_3 = 0, & \ddot{x}_3 = 0, & \ddot{x}_3 = 0, & \text{when } t = 0 \\ x_\beta = l, & \dot{x}_\beta = 0, & \ddot{x}_\beta = 0, & \ddot{x}_\beta = 0, & \text{when } t = 0 \end{array}$$

The Laplace transform of equation (14) is

$$(p^4 + \alpha p^2 + \gamma) \bar{x}_2 = \varepsilon_2 (\tau - \omega^2) \frac{p}{p^2 + \omega^2} \left(1 + e^{-\frac{\pi p}{\omega}}\right) + \varepsilon_2 p$$

$$\text{where } \varepsilon_2 = \frac{\ell \omega^2 k_1}{2(k_1 + k_2)} = \frac{T_0 \omega^2}{2(k_1 + k_2)}.$$

Thus

$$\bar{x}_2 = \varepsilon_2 \left\{ \frac{(\tau - \omega^2) p \left(1 + e^{-\frac{\pi p}{\omega}}\right)}{(p^2 + \omega^2)(p^2 + r^2)(p^2 + s^2)} + \frac{p}{(p^2 + r^2)(p^2 + s^2)} \right\}$$

$$\text{where } r^2 = \frac{\alpha + \sqrt{\alpha^2 - 4\gamma}}{2},$$

$$s^2 = \frac{\alpha - \sqrt{\alpha^2 - 4\gamma}}{2}.$$

This can be expressed as

$$\begin{aligned} \bar{x}_2 = & \varepsilon_2 (\tau - \omega^2) p \left(1 + e^{-\frac{\pi p}{\omega}}\right) \left\{ \frac{1}{(r^2 - \omega^2)(s^2 - \omega^2)(p^2 + \omega^2)} + \frac{1}{(\omega^2 - r^2)(s^2 - r^2)(p^2 + r^2)} + \right. \\ & \left. + \frac{1}{(\omega^2 - s^2)(r^2 - s^2)(p^2 + s^2)} \right\} + \\ & + \varepsilon_2 p \left\{ \frac{1}{(p^2 + r^2)(s^2 - r^2)} + \frac{1}{(p^2 + s^2)(r^2 - s^2)} \right\}. \end{aligned}$$

Hence

$$\begin{aligned} x_2 &= \frac{\ell \omega^2 k_1}{2(k_1 + k_2)} \left\{ (\tau - \omega^2) \left[\frac{\cos \omega t}{(r^2 - \omega^2)(s^2 - \omega^2)} + \frac{\cos r t}{(\omega^2 - r^2)(s^2 - r^2)} + \right. \right. \\ (0 \leq t \leq \pi/\omega) & \left. \left. + \frac{\cos s t}{(\omega^2 - s^2)(r^2 - s^2)} \right] + \right. \\ & \left. + \frac{\cos r t}{s^2 - r^2} + \frac{\cos s t}{r^2 - s^2} \right\} \\ &= \frac{\ell \omega^2 k_1}{2(k_1 + k_2)} \left\{ (\tau - \omega^2) E_1 + \frac{\cos r t}{s^2 - r^2} + \frac{\cos s t}{r^2 - s^2} \right\}. \end{aligned}$$

$$\begin{aligned}
x_2 &= \frac{e \omega^2 k_1}{2(k_1+k_2)} \left\{ (\tau-\omega^2) \left[\frac{\cos rt + \cos r \left(t - \frac{\pi}{\omega}\right)}{(\omega^2-r^2)(s^2-r^2)} + \frac{\cos st + \cos s \left(t - \frac{\pi}{\omega}\right)}{(\omega^2-s^2)(r^2-s^2)} \right] + \right. \\
&\quad \left. + \frac{\cos rt}{s^2-r^2} + \frac{\cos st}{r^2-s^2} \right\} \\
&= \frac{e \omega^2 k_1}{2(k_1+k_2)} \left\{ 2(\tau-\omega^2) \left[\frac{\cos r \left(t - \frac{\pi}{2\omega}\right) \cos \frac{r\pi}{2\omega}}{(\omega^2-r^2)(s^2-r^2)} + \frac{\cos s \left(t - \frac{\pi}{2\omega}\right) \cos \frac{s\pi}{2\omega}}{(\omega^2-s^2)(r^2-s^2)} \right] + \right. \\
&\quad \left. + \frac{\cos rt}{s^2-r^2} + \frac{\cos st}{r^2-s^2} \right\} \\
&= \frac{e \omega^2 k_1}{2(k_1+k_2)} \left\{ 2(\tau-\omega^2) E_2 + \frac{\cos rt}{s^2-r^2} + \frac{\cos st}{r^2-s^2} \right\} .
\end{aligned}$$

Similarly the Laplace transform of equation (15) is

$$(p^4 + \alpha p^2 + \gamma) \bar{x}_3 = \varepsilon_3 \frac{p}{(p^2 + \omega^2)} \left(1 + e^{-\frac{\pi p}{\omega}} \right)$$

$$\text{where } \varepsilon_3 = \frac{T_0}{2} \frac{\omega^2 k_2}{\beta m(k_1+k_2)} = \frac{e \omega^2 k_1 k_2}{2 \beta m(k_1+k_2)}$$

and hence

$$\begin{aligned}
x_3 &= \frac{e \omega^2 k_1 k_2}{2 \beta m(k_1+k_2)} E_1 \\
(0 < t < \pi/\omega) \\
x_3 &= \frac{e \omega^2 k_1 k_2}{2 \beta m(k_1+k_2)} 2 E_2 . \\
(t > \pi/\omega)
\end{aligned}$$

The Laplace transform of equation (16) is

$$(p^4 + \alpha p^2 + \gamma) \bar{x}_\beta = \frac{T_0 \gamma}{2k_1} \left\{ \frac{1}{p} \left(1 - e^{-\frac{\pi p}{\omega}} \right) + \left(1 - \frac{\omega^2}{\beta \tau} \right) \frac{p}{p^2 + \omega^2} \left(1 + e^{-\frac{\pi p}{\omega}} \right) \right\} + p^3 \ell + \alpha p \ell$$

and hence

$$\begin{aligned} x_\beta &= \frac{\ell \gamma}{2} \left\{ \frac{1}{r^2 - s^2} + \frac{1}{(r^2 - s^2)} \left(\frac{\cos rt}{r^2} - \frac{\cos st}{s^2} \right) + \left(1 - \frac{\omega^2}{\beta \tau} \right) E_1 \right\} + \\ (0 \leq t \leq \pi/\omega) & \\ & + \frac{\ell}{r^2 - s^2} (r^2 \cos rt - s^2 \cos st) - \frac{\alpha \ell}{r^2 - s^2} (\cos rt - \cos st) \end{aligned}$$

$$\begin{aligned} x_\beta &= \frac{\ell \gamma}{2} \left\{ -\frac{2}{r^2 - s^2} \left(\frac{\sin r \left(t - \frac{\pi}{2\omega} \right) \sin \frac{r\pi}{2\omega}}{r^2} - \frac{\sin s \left(t - \frac{\pi}{2\omega} \right) \sin \frac{s\pi}{2\omega}}{s^2} \right) + \right. \\ (t > \pi/\omega) & \\ & \left. + 2 \left(1 - \frac{\omega^2}{\beta \tau} \right) E_2 \right\} + \frac{\ell}{r^2 - s^2} (r^2 \cos rt - s^2 \cos st) - \\ & - \frac{\alpha \ell}{r^2 - s^2} (\cos rt - \cos st). \end{aligned}$$

APPENDIX 3

ANALYSIS OF SYSTEM IN WHICH THRUST STRUCTURE AND
LAUNCHER ONLY ARE ASSUMED FLEXIBLE

The equation of motion for this case can be obtained by putting $k_3 = \infty$ in equation (14). This gives

$$\ddot{x}_2 + \frac{k_1 k_2}{(k_1 + k_2)m} x_2 = \begin{cases} \frac{T_0}{2} \frac{\omega^2}{(k_1 + k_2)} \cos \omega t & 0 \leq t \leq \pi/\omega \\ 0 & t \geq \pi/\omega \end{cases}$$

The boundary conditions are $x_2 = \dot{x}_2 = 0$.

The Laplace transform of this equation is

$$(p^2 + n^2) \bar{x}_2 = \frac{e k_1 \omega^2}{2(k_1 + k_2)} \frac{p}{p^2 + \omega^2} \left(1 + e^{-\frac{\pi p}{\omega}} \right)$$

where $n^2 = \frac{k_1 k_2}{(k_1 + k_2)m}$,

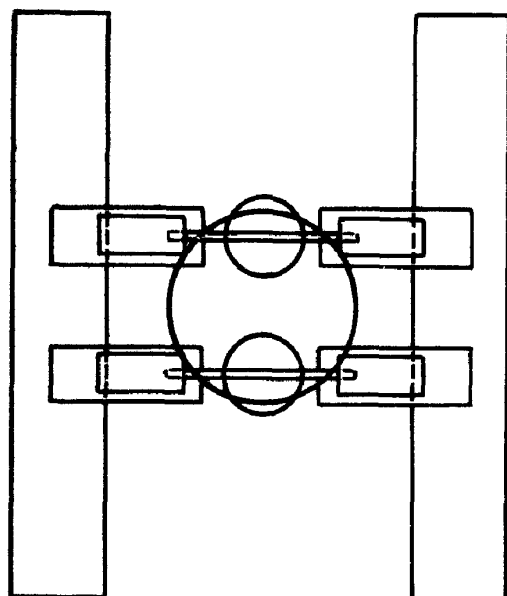
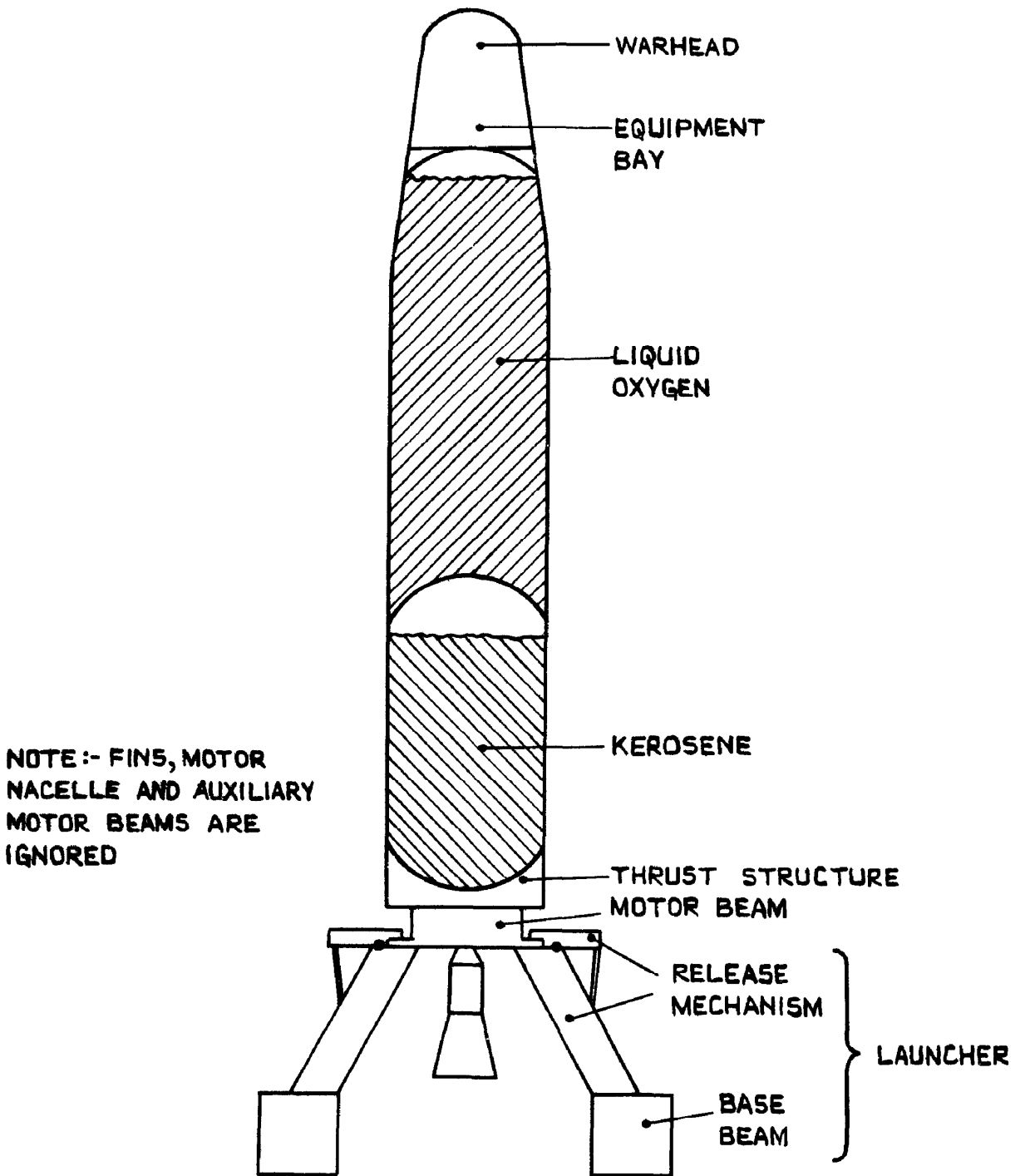
hence

$$x_2 = \frac{e k_1 \omega^2}{2(k_1 + k_2)} \left\{ \frac{\cos nt - \cos \omega t}{\omega^2 - n^2} \right\}$$

$(0 \leq t \leq \pi/\omega)$

$$x_2 = \frac{e k_1 \omega^2}{2(k_1 + k_2)} \left\{ \frac{2 \cos n \left(t - \frac{\pi}{2\omega} \right) \cos \frac{n\pi}{2\omega}}{\omega^2 - n^2} \right\}$$

$(t \geq \pi/\omega)$



PLAN VIEW OF MISSILE ON ITS LAUNCHER.
(SECTION TAKEN THROUGH THRUST STRUCTURE.)

FIG.1 SCHEMATIC DIAGRAM OF MISSILE AND LAUNCHER.

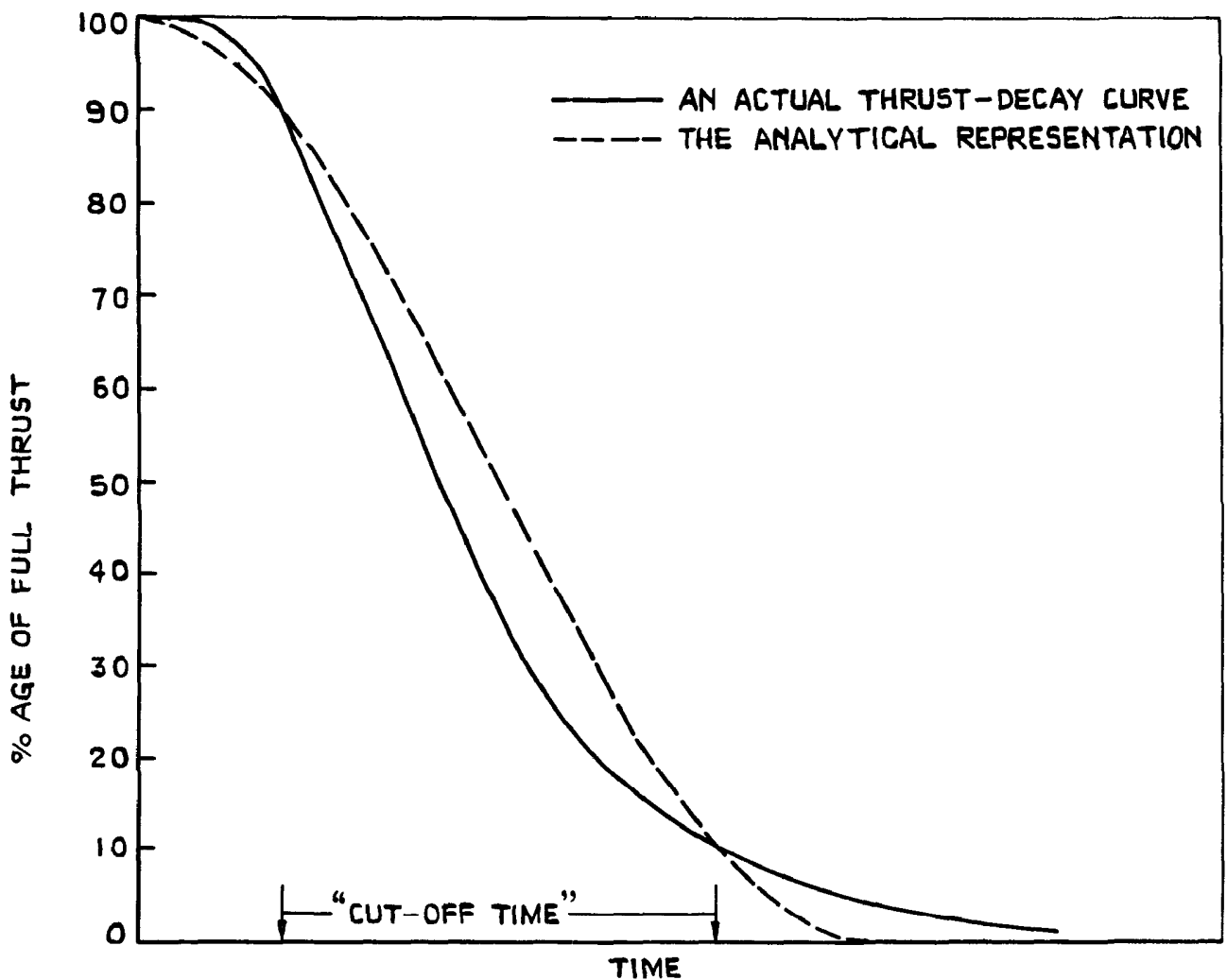


FIG. 2 COMPARISON OF AN ACTUAL THRUST-DECAY CURVE WITH THE ANALYTICAL REPRESENTATION.

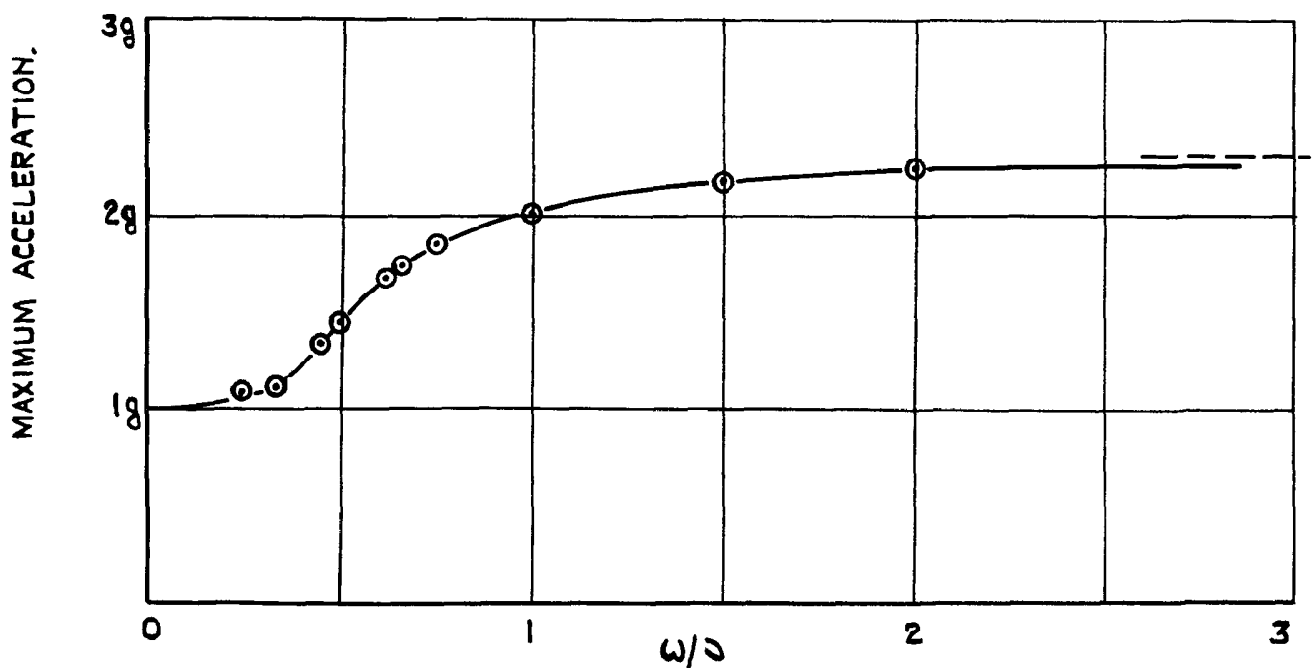


FIG. 3 MAXIMUM ABSOLUTE ACCELERATION AGAINST THE FREQUENCY RATIO ω/δ . (MISSILE RIGID.)

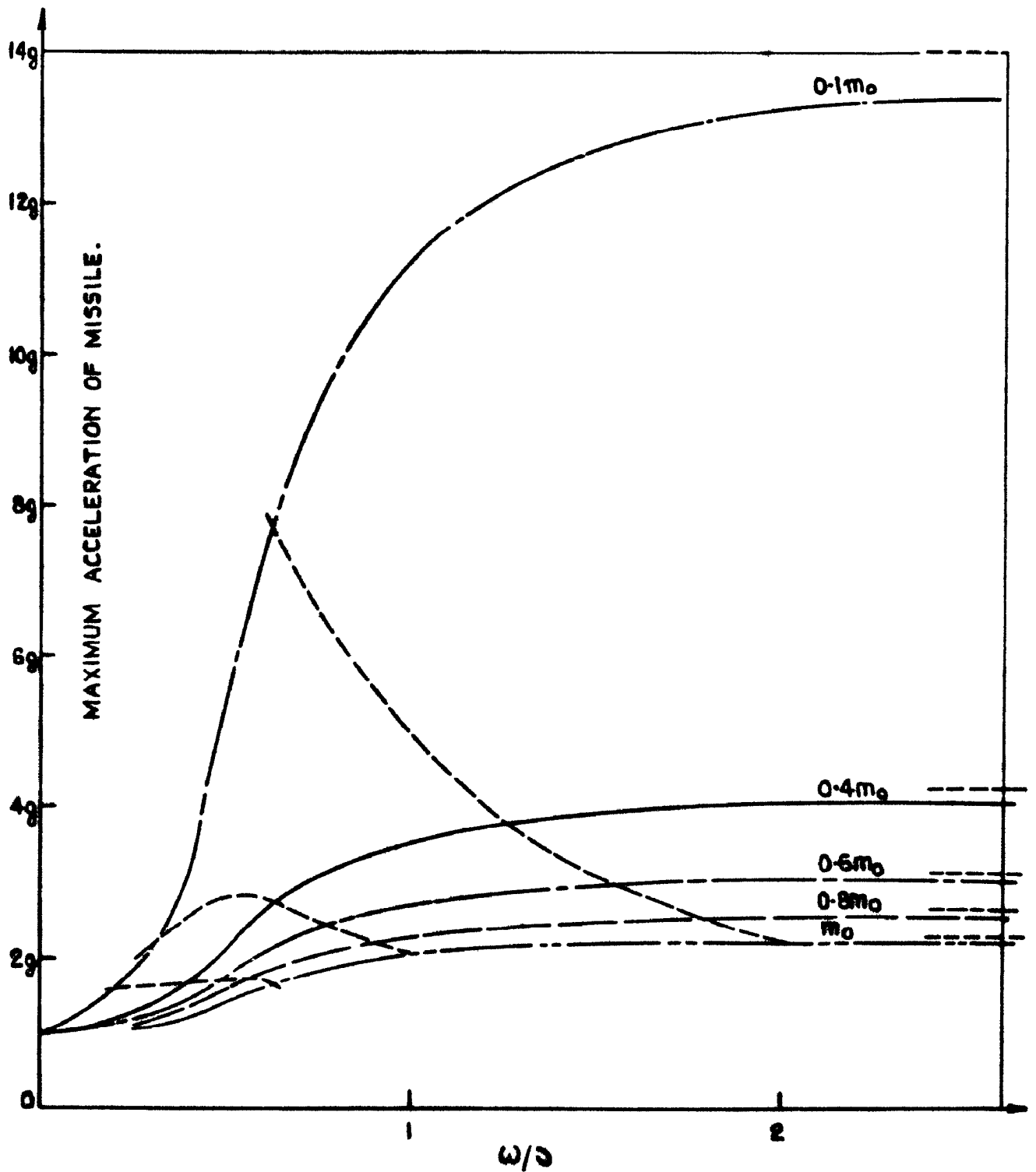


FIG.4 MAXIMUM ABSOLUTE ACCELERATION AGAINST THE FREQUENCY RATIO ω/σ ; THE EFFECT OF FUEL LOAD. (MISSILE RIGID.)

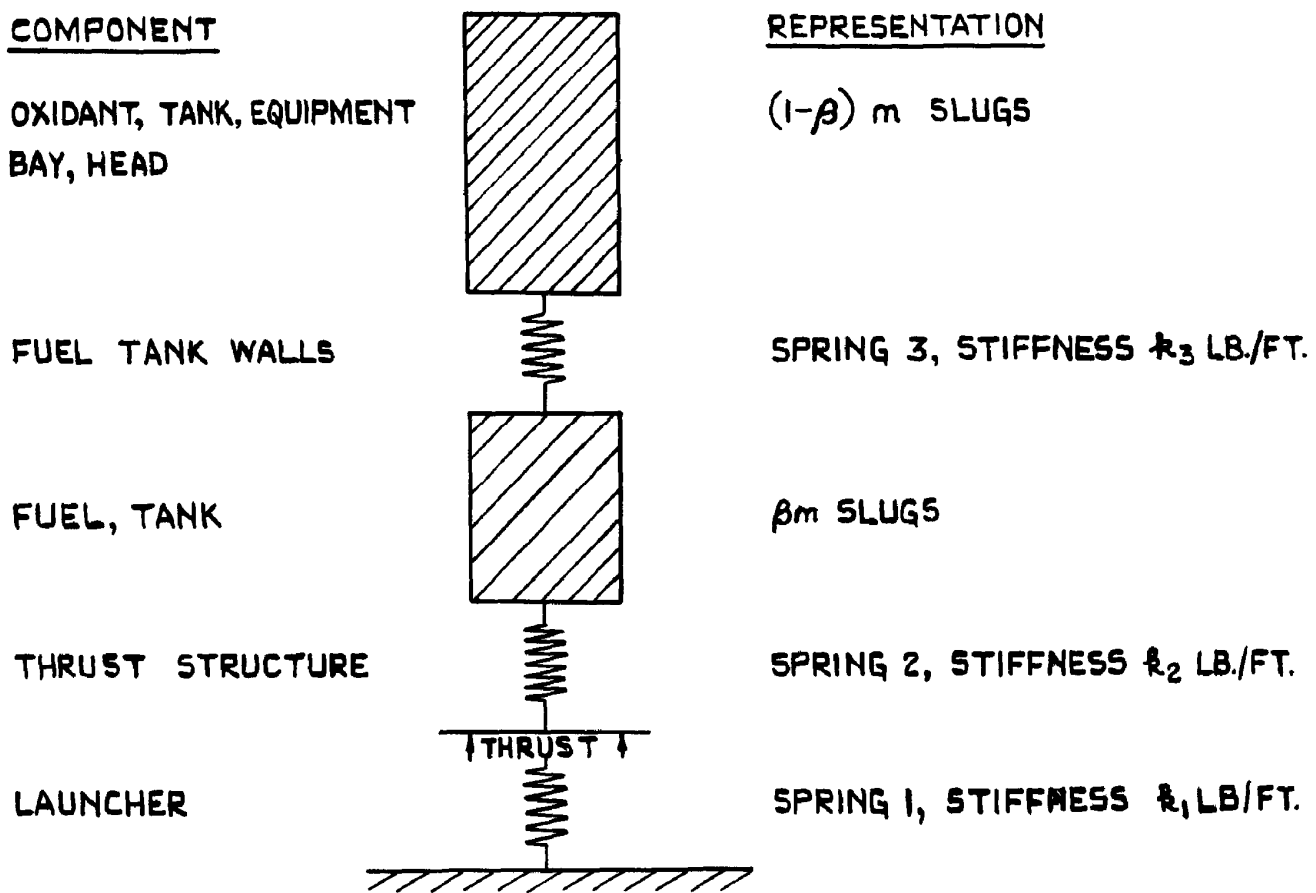


FIG. 5 MASS - SPRING REPRESENTATION OF MISSILE AND LAUNCHER.

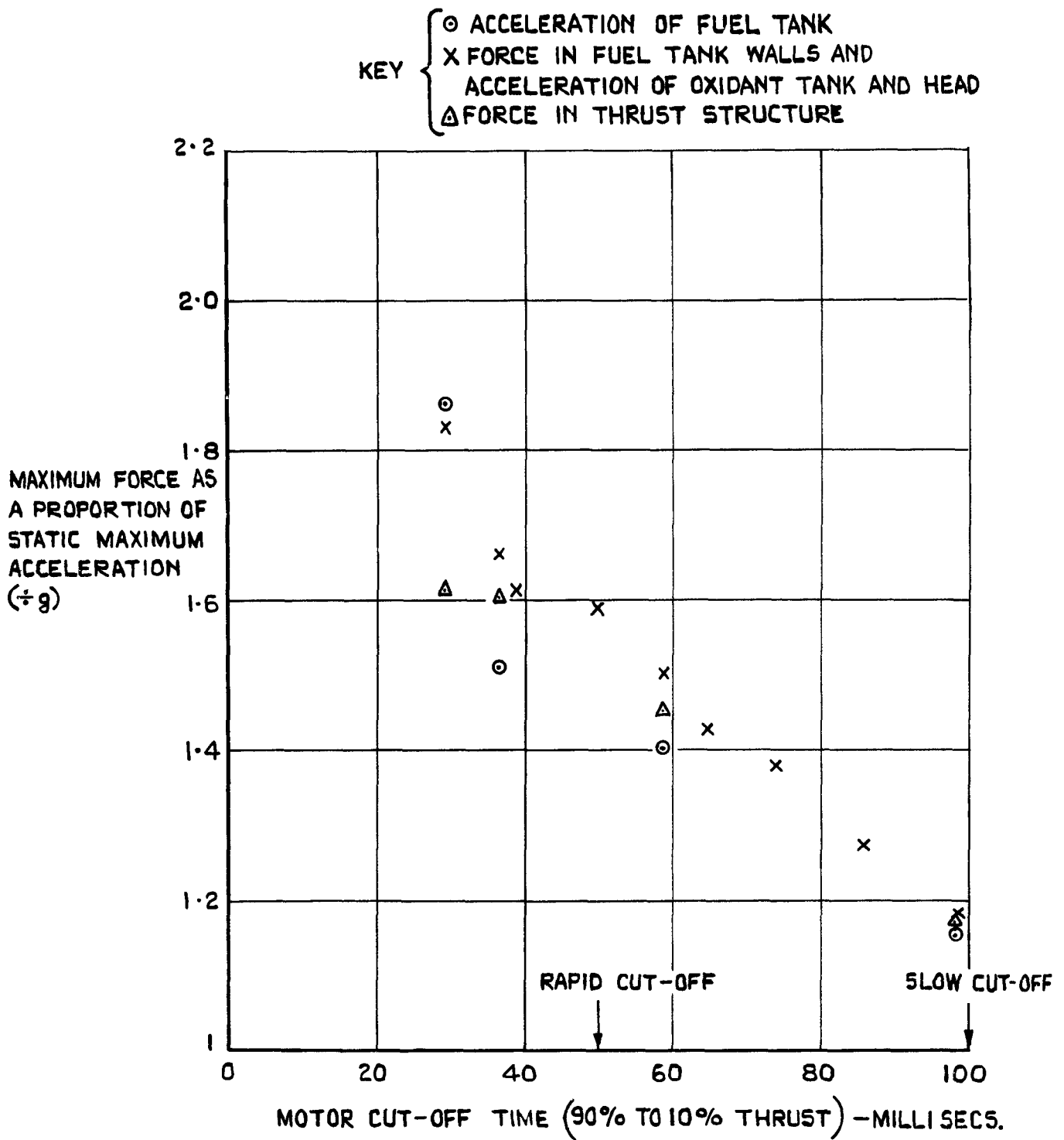


FIG.6 EFFECT OF RATE OF MOTOR CUT-OFF ON FORCES ON MISSILE. (MISSILE FLEXIBLE.)

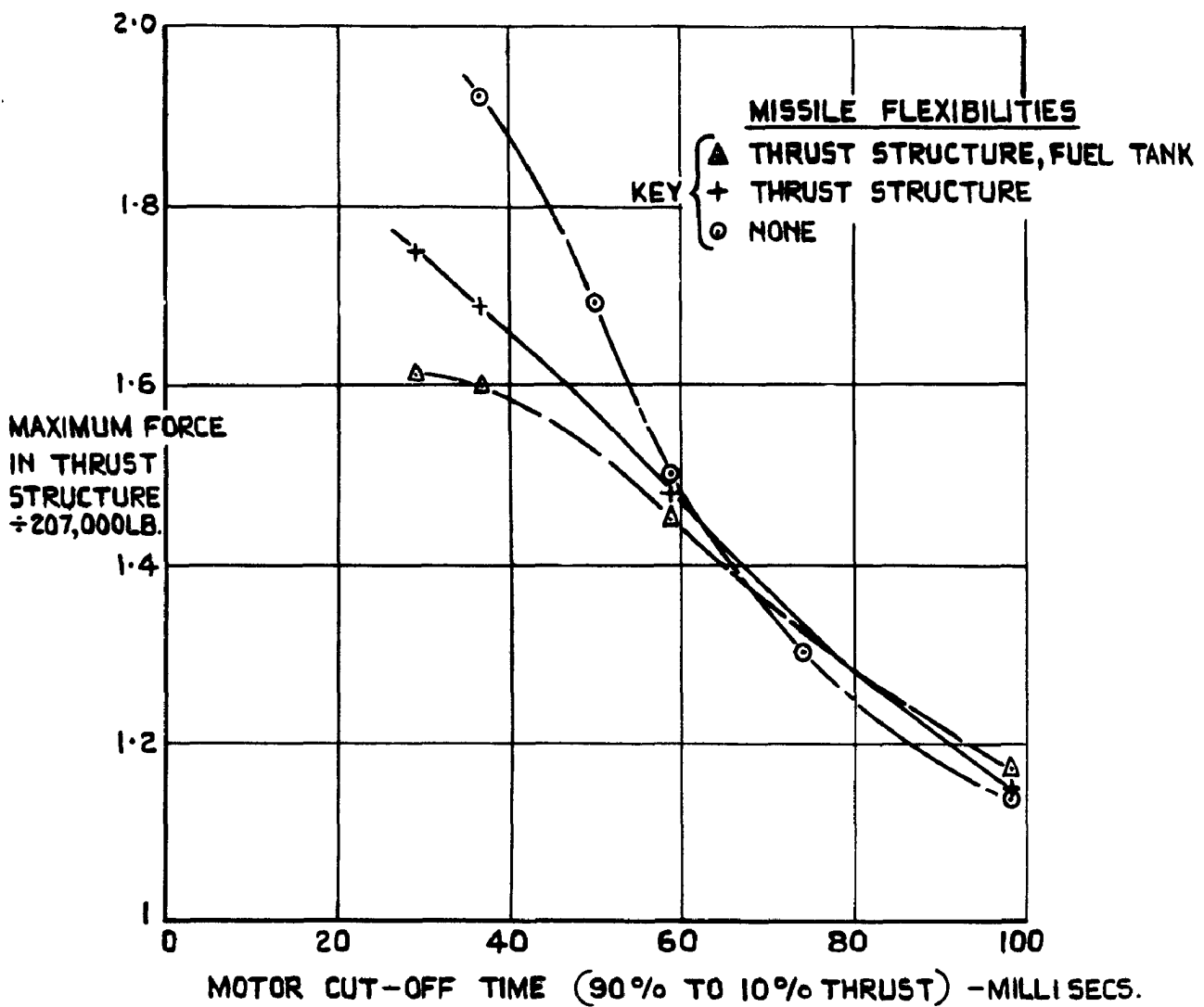


FIG. 7 EFFECT OF MISSILE FLEXIBILITIES ON MAXIMUM FORCE IN THRUST STRUCTURE.

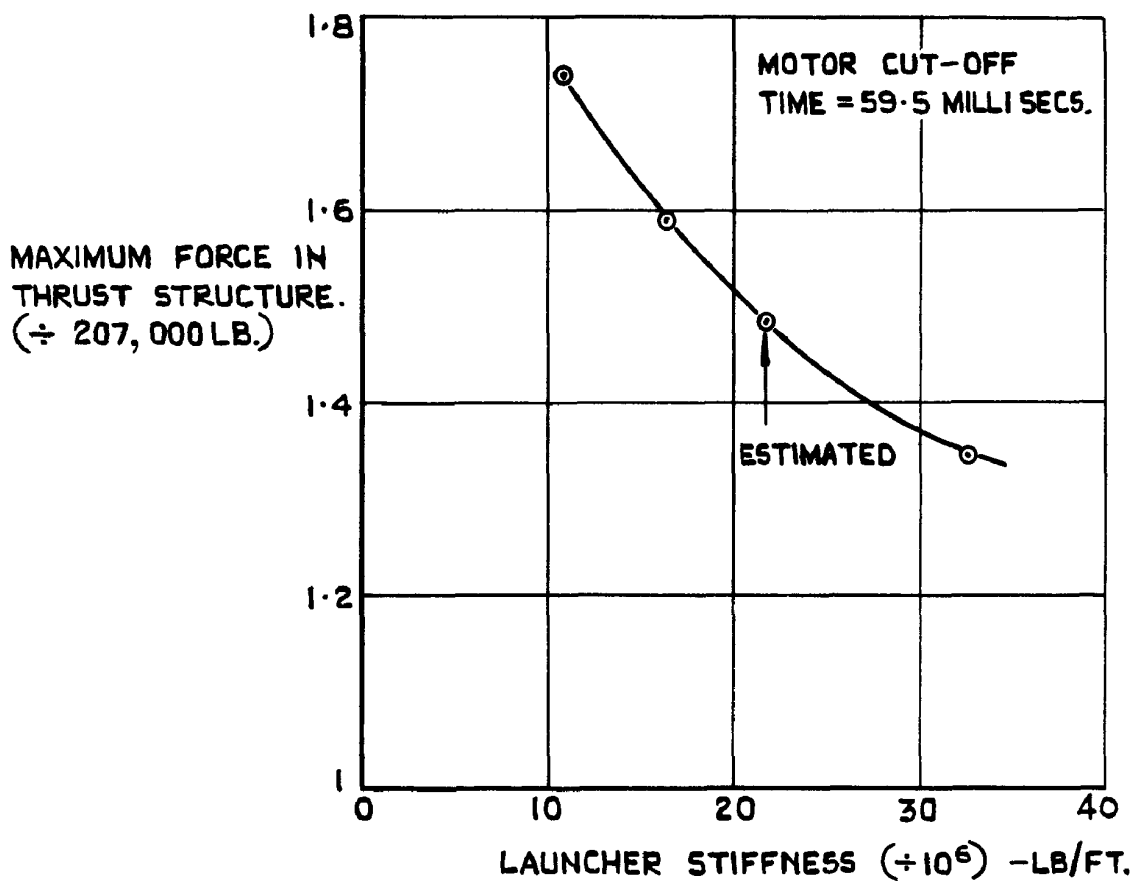


FIG. 8 EFFECT OF LAUNCHER STIFFNESS ON MAXIMUM FORCE IN THRUST STRUCTURE. (THRUST STRUCTURE FLEXIBLE, FUEL TANK WALLS RIGID.)

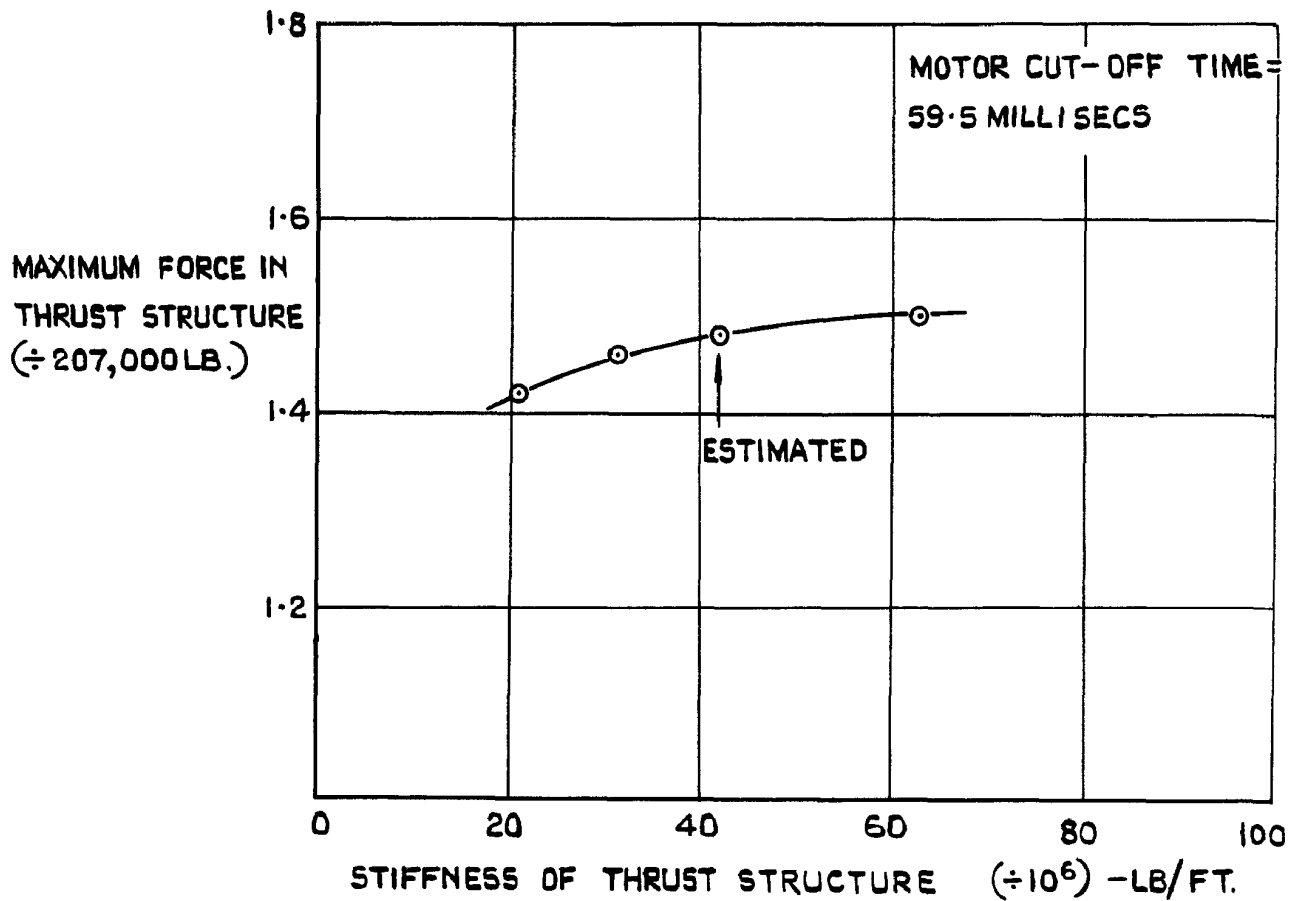


FIG. 9 EFFECT OF STIFFNESS OF THRUST STRUCTURE ON MAXIMUM FORCE IN THRUST STRUCTURE
 (THRUST STRUCTURE FLEXIBLE, FUEL TANK WALLS RIGID.)

A.R.C. C.P. No. 674

623.451-519:
533.69.048.1:
621.455.004.63

FORCES ON TETHERED BALLISTIC MISSILES DUE TO MOTOR CUT-OFF - A THEORETICAL TREATMENT. Moxon, D. August, 1960.

Motor-running tests may be carried out on a ballistic missile while it is tethered to its launcher. When the motors are cut-off the missile structure is excited in various vibration modes by the combined influence of the decaying thrust and the elastic force from the launcher. These vibrations result in loads on the missile which can exceed those encountered in normal flight. It is the magnitude of these loads and the parameters which affect them that are investigated in this paper.

The first part of the paper gives results obtained on the assumption that the missile itself is rigid while the launcher structure is elastic. This is followed by an investigation in which missile flexibility is taken into account. The results in both cases are similar; a high launcher stiffness and a low rate of thrust cut-off are found to be favourable. The effect of fuel load is studied briefly. It is found that as the fuel load decreases the overall forces decrease.

A.R.C. C.P. No. 674

623.451-519:
533.69.048.1:
621.455.004.63

FORCES ON TETHERED BALLISTIC MISSILES DUE TO MOTOR CUT-OFF - A THEORETICAL TREATMENT. Moxon, D. August, 1960.

Motor-running tests may be carried out on a ballistic missile while it is tethered to its launcher. When the motors are cut-off the missile structure is excited in various vibration modes by the combined influence of the decaying thrust and the elastic force from the launcher. These vibrations result in loads on the missile which can exceed those encountered in normal flight. It is the magnitude of these loads and the parameters which affect them that are investigated in this paper.

The first part of the paper gives results obtained on the assumption that the missile itself is rigid while the launcher structure is elastic. This is followed by an investigation in which missile flexibility is taken into account. The results in both cases are similar; a high launcher stiffness and a low rate of thrust cut-off are found to be favourable. The effect of fuel load is studied briefly. It is found that as the fuel load decreases the overall forces decrease.

A.R.C. C.P. No. 674

623.451-519:
533.69.048.1:
621.455.004.63

FORCES ON TETHERED BALLISTIC MISSILES DUE TO MOTOR CUT-OFF - A THEORETICAL TREATMENT. Moxon, D. August, 1960.

Motor-running tests may be carried out on a ballistic missile while it is tethered to its launcher. When the motors are cut-off the missile structure is excited in various vibration modes by the combined influence of the decaying thrust and the elastic force from the launcher. These vibrations result in loads on the missile which can exceed those encountered in normal flight. It is the magnitude of these loads and the parameters which affect them that are investigated in this paper.

The first part of the paper gives results obtained on the assumption that the missile itself is rigid while the launcher structure is elastic. This is followed by an investigation in which missile flexibility is taken into account. The results in both cases are similar; a high launcher stiffness and a low rate of thrust cut-off are found to be favourable. The effect of fuel load is studied briefly. It is found that as the fuel load decreases the overall forces decrease.

© *Crown copyright* 1964

Printed and published by

HER MAJESTY'S STATIONERY OFFICE

To be purchased from

York House, Kingsway, London w.c.2

423 Oxford Street, London w.1

13A Castle Street, Edinburgh 2

109 St. Mary Street, Cardiff

39 King Street, Manchester 2

50 Fairfax Street, Bristol 1

35 Smallbrook, Ringway, Birmingham 5

80 Chichester Street, Belfast 1

or through any bookseller

Printed in England